Conical vortices: A class of exact solutions of the Navier–Stokes equations[a)]

C.-S. Yih and F. Wu[b)]
University of Michigan, Ann Arbor, Michigan 48103

A. K. Garg and S. Leibovich
Sibley School of Mechanical and Aerospace Engineering, Cornell University, Ithaca, New York 14853

(Received 23 February 1982; accepted 8 September 1982)

A two-parameter family of exact axially symmetric solutions of the Navier–Stokes equations for vortices contained within conical boundaries is found. The solutions depend upon the same similarity variable, equivalent to the polar angle ϕ measured from the symmetry axis, as flows previously discussed by Long and by Serrin, but are distinct from the cases they treated. The conical bounding stream surfaces of the present solution can be located at any angle $\phi = \phi_0$, where $0 < \phi_0 < \pi$. The flows in all of these cases, when solutions exist, are finite everywhere except at the cone vertex which is a source of axial momentum, but not of volume. Solutions are of three types, flow may be (a) towards the vertex on the axis and away from the vertex at the conical boundary, (b) towards the vertex both on the axis and at the cone, or (c) away from the vertex on the axis and towards it at the bounding cone. In the first and second case, strong shear layers form on the cone walls for high Reynolds numbers. In case (c), a region of strong axial shear and strong axial vorticity forms near the axis, even for low Reynolds numbers. The qualitative nature of the possible solutions is deduced, using methods of argument due to Serrin, and examples of flows are numerically computed for cone half-angles of $\pi/4$, $\pi/2$ (flows above the plane $z = 0$), and $3\pi/4$. Regions of the parameter space where solutions are proven not to exist are given for the cone half-angles given above, as well as regions where solutions are proven to exist.

I. INTRODUCTION

Known exact solutions of the Navier–Stokes equations representing steady axially symmetric flows with swirl fall into three classes. One class constitutes those solutions for which radial component u and the azimuthal component v of the velocity vector expressed in cylindrical (r,θ,z) coordinates are allowed to depend only upon r (time dependence may also be permitted). This class has been explored by Donaldson and Sullivan[1]; special cases had been discovered earlier by Burgers[2] and by Rott,[3] and has been further considered by Bellamy-Knights.[4,5] A second interesting class, not in similarity form, represents vortices with arbitrary stream surfaces for which the azimuthal velocity $v = \lambda r^{-1}\psi$, and the azimuthal vorticity $\zeta = \lambda v$, where λ is a constant and ψ is the Stokes stream function. The swirl components of these flows, which were discovered by Trkal[6] (cf. Berker[7]) decay like $\exp(-\nu\lambda^2\tau)$, where ν is the kinematic viscosity, and the asymptotic states are axially symmetric irrotational flows. The third class of exact solutions is that considered here, the "conical" vortices.

It is easy to show (see Sec. II) that solutions of the conical form are the only similarity solutions allowing the azimuthal velocity to vary along the axis of symmetry. This class of flows is the generalization of the Landau–Squire[8–11] round jet to permit an azimuthal component of the velocity. The first work on conical vortices apparently can be traced to Loitsianskii[12] (in a boundary-layer approximation) and, independently, to Long.[13]

Many different flows are embraced by this conical form depending upon the conditions imposed on the solution of the similarity equations. Long[13] imposed the condition that the circulation, Γ, about the axis tend to a constant as $r\rightarrow\infty$, where r is the cylindrical radius. In addition, but without explicitly stating so, he imposed the condition that the flow be symmetric in z. This can be interpreted either as a symmetric flow with a sheet of sources of variable strength on the plane $z = 0$, or as a continuous flow with a porous wall at $z = 0$ with a prescribed variable normal velocity. The flow in either event is smooth in the upper half plane, and numerical solutions to a boundary-layer approximation of the governing equations have been given by Long[14] and by Burggraf and Foster.[15] These solutions are very interesting and represent vortices concentrated near the symmetry axis that closely resemble vortices observed in laboratory experiments.

Serrin[16] has given a complete mathematical treatment of a subclass of conical vortices representing flow above the plane $z = 0$. A special case of this subclass had earlier been discussed by Goldstik.[17] The no-slip condition was imposed on the plane, and $\Gamma\rightarrow$const as $r\rightarrow 0$. Thus, this subclass represents the flow of a line vortex above a plane and a singularity is accepted on the axis $r = 0$.

In this paper, we consider the subclass of flows which are contained within a cone with vertex at the origin and axis

[a)] This paper is an amalgamation of two independent efforts. The first, by Yih and Wu, dealt with flows above a plane surface, and was completed some months before the second, by Garg and Leibovich, which dealt with the same problem, but in the context of general conical boundaries. The methods used in the two papers were slightly different, but mathematically equivalent.

[b)] Permanent address: Chinese Univ. of Science and Technology, Hofei, People's Republic of China.

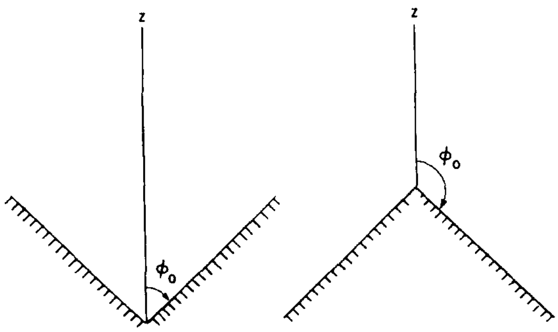

FIG. 1. Flow region.

the positive z axis, as shown in Fig. 1; the cone half-angle may exceed $\pi/2$. We require that solutions yield finite velocity except at the vertex of the cone, where a singularity is inevitable. In addition, we require the conical boundaries of the flow to be stream surfaces. The solutions are therefore distinct from those previously found. As in the various cases of the nonswirling exact axisymmetric solutions,[8–11] it is not possible to satisfy the no-slip condition on stream surfaces. This difficulty is discussed in the final section of the paper.

The solutions explored constitute a two parameter family, the parameters being a Reynolds number (defined as $\Gamma/4\pi\nu$, where Γ is a characteristic circulation about the symmetry axis), and a number representing the net momentum flux issuing from the vertex of the cone. The qualitative behavior and existence of this two-parameter family of solutions is explored using methods developed by Serrin,[16] Weyl,[18] together with modifications which appear to be necessary for this problem. Regions of the parameter space in which solutions exist, as well as regions in which solutions fail to exist, are delineated.

We then construct some examples of flows in this class by numerical integration of the governing equations, again following the lead of Serrin and of Weyl. Boundary layers can develop either on the axis or on the bounding conical stream surface, depending upon the choice of parameters. An interesting feature is that strong shear develops at low Reynolds number for some values of the second controlling parameter. Our numerical examples include a number of flows existing above the plane $z = 0$, and one each for flows within cones with half angles of $\pi/4$ and $3\pi/4$, respectively.

II. CONICAL SIMILARITY

In this section, we give a brief demonstration that conical vortices are, in fact, the only similarity form of the axially symmetric Navier–Stokes equations that yield both finite velocities at the axis and at arbitrarily great distances along the axis and perpendicular to it.

The steady axially symmetric Navier–Stokes equations in cylindrical coordinates (r,θ,z), with velocity components (u,v,w), may be written in the form

$$uK_r + wK_z = \nu D^2K,$$
$$u\zeta_r + w\zeta_z - 2ur^{-1}\zeta - 2r^{-2}KK_z = \nu D^2\zeta,$$
$$\zeta = -D^2\psi, \quad w = r^{-1}\psi_r,$$
$$u = -r^{-1}\psi_z, \quad v = r^{-1}K,$$
$$D^2(\ ) = (\ )_{rr} - r^{-1}(\ )_r + (\ )_{zz}.$$

Here $2\pi K(r,z)$ is the circulation about the z axis, ζ is the azimuthal vorticity, and ν is the kinematic viscosity.

This set is invariant under the change of scale

$$r = ar', \quad z = bz', \quad \psi(r,z) = c\psi'(r',z'),$$
$$K(r,z) = \gamma K'(r',z')$$

in three cases

$$\text{(I)}\ a = b, \ \gamma = 1,$$
$$\text{(II)}\ \gamma_{zz} = K_{zz} = 0,$$
$$\text{(III)}\ r\frac{\partial}{\partial r}\frac{1}{r}\frac{\partial\psi}{\partial r} = r\frac{\partial}{\partial r}\frac{1}{r}\frac{\partial K}{\partial r} = 0.$$

Case (II) admits solutions of the form

$$w = zw_1(r) + w_2(r), \quad u = u_1(r), \quad v = v_1(r),$$

which is a generalized form of the similarity assumed by Burgers,[2] Rott,[3] and Donaldson and Sullivan.[1] Case (II) can be further reduced to the problems considered by these authors, since the problem for $w_2(r)$ can be solved separately once $u_1(r)$, $v_1(r)$ and $w_1(r)$ are known.

In case (III), all solutions are of the form

$$w = w(z), \quad u = rw'(z) + u_2(z)/r, \quad v = r\omega(z) + v_2(z)/r.$$

With $u_2 = v_2 = 0$, the classical Kármán[19] or Bödewadt[20] forms for flow above a rigidly rotating plane or rigidly rotating flow above a stationary plane are obtained.

Case (I) leads to solutions of the form

$$K(r,z) = K(\eta), \quad \psi = zG(\eta), \quad \eta = r/z,$$

or

$$v = r^{-1}K(\eta), \quad u = -r^{-1}G(\eta), \quad w = z^{-1}G'(\eta).$$

The similarity variable is $\eta = r/z = \tan\phi$, where ϕ is the polar angle in spherical coordinates. There is, in addition, an unsteady version with this spatial symmetry. If time dependence is allowed, the functions K, and G depend upon $z^2/\nu\tau$ as well as η.

Case (I) admits solutions with the velocity field finite everywhere except for the origin $r = z = 0$. In cases (II) and (III), the velocities can be finite at the axis, but approach infinity as either r or z approaches infinity.

III. FORMULATION OF THE PROBLEM FOR CONICAL FLOWS

The equations of motion for conical similarity assume a more compact form when expressed in spherical coordinates, since the similarity variable is then simply the polar angle.

Thus, we adopt spherical coordinates (R,ϕ,θ), where R is the distance from the origin, ϕ is the polar angle, measured from the positive z axis, and θ is the azimuthal angle. Serrin[16] has presented the appropriate equations for the problem. Let the velocity vector be (v_R, v_ϕ, v_θ), then the similar solutions are in the form

$$v_R = \frac{\widetilde{F}'(x)}{R}, \quad v_\phi = \frac{\widetilde{F}(x)}{r}, \quad v_\theta = \frac{\widetilde{\Omega}(x)}{r}, \tag{1}$$

where

$$r = R \sin \phi$$

is the cylindrical radius, and

$$x = \cos \phi. \qquad (2)$$

Continuity is satisfied by the form (1). In terms of x, $\widetilde{F}$ and $\widetilde{\Omega}$ must satisfy the pair of ordinary differential equations

$$\nu(1 - x^2)\widetilde{F}^{iv} - 4\nu x\widetilde{F}''' + \widetilde{F}\widetilde{F}''' + 3\widetilde{F}'\widetilde{F}''$$
$$= -2\widetilde{\Omega}\widetilde{\Omega}'/(1 - x^2), \qquad (3a)$$

$$\nu(1 - x^2)\widetilde{\Omega}'' + \widetilde{F}\widetilde{\Omega}' = 0. \qquad (3b)$$

The pressure can be recovered, knowing $\widetilde{F}$ and $\widetilde{\Omega}$, from the relation

$$\frac{p}{\rho} = \frac{\widetilde{\Pi}(x)}{r^2} + \frac{p_\infty}{\rho}, \qquad (3c)$$

$$-2\widetilde{\Pi} = \widetilde{F}^2 + \widetilde{\Omega}^2 + \{\widetilde{F}\widetilde{F}'' + \widetilde{F}'^2 + \nu[(1 - x^2)\widetilde{F}'''$$
$$- 2x\widetilde{F}'']\}(1 - x^2), \qquad (3d)$$

where p_∞ is the pressure at $r = \infty$.

The problem is therefore reduced to finding $\widetilde{F}$ and $\widetilde{\Omega}$ from (3) and appropriate boundary conditions.

A. Boundary conditions

Let the fluid be confined within an impenetrable cone with vertex at the origin and with the positive z axis ($x \equiv 1$) as axis. The cone semi-angle may be larger than $\pi/2$, so the flow region may include the entire space, excluding the negative z axis, if desired. Let $x = x_0$ ($-1 < x_0 < 1$) be the cone boundary. Then the boundary conditions are taken to be

$$2\pi\widetilde{\Omega}(x_0) = \Gamma, \qquad (4a)$$

$$\widetilde{F}(x_0) = 0, \qquad (4b)$$

$$\widetilde{F}(1) = 0, \qquad (4c)$$

$$\lim_{x \to 1}(1 - x^2)\widetilde{F}''(x) = 0, \qquad (4d)$$

$$\widetilde{\Omega}(1) = 0. \qquad (4e)$$

Condition (4a) establishes the existence and level of the swirl, and, without loss of generality, we take $\Gamma > 0$. Condition (4b) states that the normal velocity on the cone $x = x_0$ vanishes. Condition (4c) ensures that v_ϕ be finite and that the axis is not a source of mass. Condition (4d) ensures finite acceleration on any finite length needle of fluid on the z axis due to the viscous forces, and assures that the radial velocity [i.e., $F'(1)$] is finite as well. The limiting condition must be imposed due to the singularity at $x = 1$ associated with the coordinate system. Condition (4e) requires the azimuthal velocity to be finite at the axis.

If we now let

$$2\pi\widetilde{\Omega}(x) = \Gamma\Omega(x), \quad \widetilde{F} = \nu F, \quad \widetilde{\Pi} = \nu^2\Pi, \qquad (5)$$

and define the Reynolds number

$$\mathrm{Re} = \Gamma/4\pi\nu,$$

then the system assumes the dimensionless form

$$(1 - x^2)F^{iv} - 4xF''' + FF''' + 3F'F''$$
$$= 4\,\mathrm{Re}^2(-2\Omega\Omega'/1 - x^2), \qquad (6a)$$

$$(1 - x^2)\Omega'' + F\Omega' = 0, \qquad (6b)$$

$$-2\Pi(x) = F^2 + (1 - x^2)\{FF'' + F'^2 + (1 - x^2)F'''$$
$$- 2xF''\} + 4\,\mathrm{Re}^2\,\Omega^2, \qquad (6c)$$

and the boundary conditions (4) apply to the dimensionless variables, provided $\Gamma/2\pi$ is replaced by unity.

B. Reduction to an integro-differential equation

Equation (6a) can be integrated three times to give (cf. Ref. 16)

$$2(1 - x^2)F' + 4xF + F^2 = 4\,\mathrm{Re}^2\,G(x), \qquad (7a)$$

where

$$G(x) = -\int_{x_0}^{x} dt_2 \int_{x_0}^{t_2} dt_1 \int_{x_0}^{t_1} \frac{4\Omega\Omega'\,dt}{1 - t^2} + Ax^2 + Bx + C. \qquad (7b)$$

The boundary conditions (4c) and (4d) show that $G(1) = G'(1) = 0$. Application of these two conditions allows us to eliminate B and C in favor of A. Upon integration by parts and rearrangement, we can place G in the form

$$G(x) = 2(1 - x)^2 \int_{x_0}^{x} \frac{t\Omega^2\,dt}{(1 - t^2)^2}$$
$$+ 2x\int_x^1 \frac{\Omega^2\,dt}{(1 + t)^2} + T(1 - x)^2, \qquad (8)$$

where

$$T = A + 1/(1 - x_0^2),$$

and we adopt T as the basic parameter instead of A.

We will need to know the properties of $G(x)$; for later reference, we note that the first and second derivatives of G are

$$G'(x) = -4(1 - x)\int_{x_0}^{x} \frac{t\Omega^2\,dt}{(1 - t^2)^2}$$
$$+ 2\int_x^1 \frac{\Omega^2\,dt}{(1 + t)^2} - 2T(1 - x), \qquad (9)$$

and

$$G''(x) = 4\int_{x_0}^{x} \frac{t\Omega^2\,dt}{(1 - t^2)^2} - \frac{2\Omega^2(x)}{1 - x^2} + 2T. \qquad (10)$$

Thus, $G'(1) = 0$, and $G''(1)$ is finite provided $\Omega(x) = O(1 - x)$ as $x \to 1$.

Using (9) and (10), one can reduce the pressure function $\Pi(x)$ in (6c) to the simpler form (cf. Ref. 16)

$$-2\Pi(x) = 4xF + 2F^2 - 4\,\mathrm{Re}^2\,xG'(x). \qquad (11)$$

A similar formula allowed Serrin[16] to relate the parameter analogous to T to the pressure level on the wall. In our case, (11) evaluated at the cone $x = x_0$ gives

$$\Pi(x_0) = 4\,\mathrm{Re}^2\,x_0\left(\int_{x_0}^1 \frac{\Omega^2\,dt}{(1 + t)^2} - T(1 - x_0)\right). \qquad (12)$$

On the axis, (11) reveals that

$$\Pi(1) = 0$$

so that the pressure on the axis equals p_∞. Thus T can be related to the wall pressure through (12) for $x_0 \neq 0$, but the connection is less direct than in Serrin's case.

The similarity relations (1) coupled with the boundary conditions (4b,4c) imply that the singular point at the origin is not a source of volume, but it is a source of axial momentum. The axial momentum flux issuing from the origin is

$$M = 2\pi\rho\nu^2 \int_{x_0}^{1} xF'^2\, dx. \quad (13)$$

The nondimensionalized momentum flux $M/\rho\nu^2$ is a function of the parameters Re and T.

In the present case the integrand is everywhere finite. In Serrin's case, the integrand is infinite at $x = 1$, but it, too, is integrable.

We conclude this section by introducing the change of variable[16]

$$F(x) = 2(1 - x^2)f(x), \quad (14)$$

which puts (6a) and (6b) in the final form to be considered

$$f' + f^2 = \mathrm{Re}^2[G(x)/(1 - x^2)^2], \quad (15)$$

$$\Omega'' + 2f\Omega' = 0, \quad (16)$$

subject to the conditions

$$\Omega(x_0) = 1, \quad f(x_0) = 0, \quad \Omega(1) = 0. \quad (17)$$

IV. QUALITATIVE BEHAVIOR OF SOLUTIONS

Equation (16) can be integrated, assuming f to exist and treating it as known; the result is

$$\Omega'(x) = \Omega'(x_0) \exp\left(-2\int_{x_0}^{x} f\,dx \right). \quad (18)$$

Thus $\Omega'(x)$ is one-signed in $(x_0, 1)$, and $\Omega(x)$ is monotonic. Since $\Omega(1) = 0$ and $\Omega(x_0) = 1$, $\Omega'(x_0) < 0$.

Next, consider the behavior of the solution near $x = 1$. Since the argument above shows that

$$0 \leqslant \Omega(x) \leqslant 1,$$

we can derive upper and lower bounds on $G(x)$ by substituting either $\Omega = 0$ or $\Omega = 1$ in the integrals in (8). The choice of 0 or 1 depends upon which bound is being sought and, in considering that bound, whether the contribution of the terms involving integrals is positive or negative. For example, when calculating an upper bound for $x_0 < 0$, we set $\Omega = 0$ in both integrals of (8) when $x < 0$ and $\Omega = 1$ when $x > 0$. In this way, after minor manipulations, we arrive at the bounds

$$(1-x)^2\left(T + \frac{xI(-x)I(-x_0)}{1-x} - \frac{x_0^2 I(-x_0)}{1-x_0^2}\right)$$
$$\leqslant G(x) \leqslant (1-x)^2\left(T + \frac{xI(x)}{1-x} - \frac{x_0^2 I(x_0)}{1-x_0^2}\right), \quad (19)$$

where the function $I(x)$ is the unit function, $I(x) = 1$ for $x > 0$, $I(x) = 0$, $x \leqslant 0$.

Under similar conditions on G, Serrin[16] has proved that

$$f = O\{\ln[1/(1-x)]\} \quad \text{as } x \to 1, \quad (20)$$

hence, from (18) $\Omega'(1)$ is finite, and his proof follows without change if G satisfies (19). Therefore

$$\Omega(x) = O(1 - x)$$

near $x = 1$, and this in turn shows that the functions

$$\int_{x_0}^{x} \frac{t\Omega^2}{(1-t^2)^2}\,dt, \quad \frac{\Omega^2(x)}{(1-x^2)}$$

are finite as $x \to 1$. Consequently

$$G(1) = G'(1) = 0, \quad G''(1) = 4\int_{x_0}^{1} \frac{t\Omega^2\,dt}{(1-t^2)^2} + 2T < \infty, \quad (21)$$

and we can consequently replace (19) by the stronger statement: the function

$$H(x) = \mathrm{Re}^2[G(x)/(1-x^2)^2] \quad (22)$$

is finite for all $x_0 < x < 1$. Furthermore, from (8) and (22), we observe that

$$\frac{d}{dx}[(1+x)^2 H(x)] = 2\,\mathrm{Re}^2 \frac{(1+x)}{(1-x)^3} \int_x^1 \frac{\Omega^2\,dt}{(1+t)^2}. \quad (23)$$

Since $\Omega = O(1-x)$ near $x = 1$, the integral in (23) is finite for all x in the interval I: $\{x_0 \leqslant x \leqslant 1, x_0 > -1\}$. Thus,

$$\frac{d}{dx}[(1+x)^2 H(x)] > 0 \quad (24)$$

in I. We infer from this that if $H(x)$ is positive at any point $x = x_1$, then it remains positive for all $x > x_1$. In particular, if $H(x_0) > 0$, then $H > 0$ throughout the interval I. If $H(x_0) < 0$, then $H(x)$ can change sign at most once. In this case, either

$H(x) < 0$ in I, or

$H(x) < 0$ for $x_0 \leqslant x < x_1 < 1$, and

$H(x) \geqslant 0$ for $x_1 \leqslant x \leqslant 1$.

Following Serrin[16] we write (15) in the easily verified form

$$f(x) = \int_{x_0}^{x} H(t) \exp\left(-\int_t^x f(u)du \right) dt, \quad (25)$$

where the boundary condition $f(x_0) = 0$ has been applied. In view of the properties of $H(x)$, (25) shows that $f \geqslant 0$ in I if $H(x_0) > 0$. Furthermore, if $H(x) < 0$ for $x_0 \leqslant x < x_1 \leqslant 1$, then either (i) $f < 0$, $f' < 0$ for all x in I, or (ii) $f \leqslant 0$ for $x_0 \leqslant x < x_2 \leqslant 1$, where $x_2 > x_1$, and $f > 0$ for $x_2 < x \leqslant 1$. Thus, if $H(x_0) < 0$, either f is negative everywhere in the cone, or it is negative in a sector near $x = x_0$, and positive in the remainder of the cone: it may pass through zero no more than once. We may immediately determine this behavior in some instances. The lower bound of (19) is non-negative when

$$T \geqslant \max[0, -x_0/(1-x_0^2)], \quad (26)$$

and therefore $H(x) > 0$, $f(x) \geqslant 0$ for these values of T. Furthermore, $H(x_0) < 0$, implying $f(x) < 0$ in at least a sector near $x = x_0$, when

$$T < \min[0, -x_0/(1-x_0^2)]. \quad (27)$$

Thus, for the case of a plane surface, $T = 0$ is the critical parameter dividing fully positive solutions from mixed or fully negative solutions. For other values of x_0, the specification of T does not completely resolve this issue *a priori*, since the critical value of T dividing fully positive solutions from mixed or negative ones lies in a gap between (26) and (27). In these cases we can only say, *a priori*, that there is a critical value of T, denoted T^*, where

$$\max[0, -x_0/(1-x_0^2) < T^* < \min(0, -x_0/(1-x_0^2)], \quad (28)$$

such that fully positive solutions obtain when $T \geqslant T^*$ and mixed or fully negative solutions obtain for $T < T^*$.

A solution to the fluid-dynamical problem exists only if $(1 - x^2)f(x)$ is finite. Thus f must be finite for all $x_0 < x < 1$, but singularity in f with $f = O(1/1 - x)$ is permissible as $x \to 1$. Indeed, we have already cited Serrin's result (20) which shows that f, if it exists, can be no more singular than the logarithm. These arguments assume the existence of a solution, however, and it will be shown in the next section that there are no solutions to our problem for certain combinations of parameters, just as in Ref. 16. We may go one step further, if solutions exist: then we have already argued that f is integrable, thus, in view of (22), (23) shows that f is finite everywhere in the cone.

We may now summarize and sketch the general features of the flows. We have found that, if solutions exist:

(1) f is finite, and $\Omega' \leqslant 0$;

(2) (a) There is a number T^*, partially determined by (28) such that f is non-negative and (from (18)) $\Omega'' \geqslant 0$, for $T \geqslant T^*$, and

(3) (b) If $T < T^*$, then f will be negative and $\Omega'' < 0$ in an interval $x_0 < x < x_1 \leqslant 1$, and $f \geqslant 0$ and $\Omega'' \geqslant 0$ in $x_1 \leqslant x \leqslant 1$.

Since

$$Rv_R = 2[H(x)(1 - x^2) - (1 - x^2)f^2 - 2xf], \tag{29}$$

at the axis $x = 1$,

$$Rv_R = -4f(1), \tag{30}$$

and at $x = x_0, f(x_0) = 0$, and

$$Rv_R = 2H(x_0)(1 - x_0^2). \tag{31}$$

Case (a) above therefore has $v_R < 0$ on the axis, and $v_R > 0$ at the conical boundary [since this case corresponds to $H(x_0) \geqslant 0$]. In case (b), either $f \leqslant 0$ throughout, or $f < 0$ near $x = x_0$ and $f > 0$ near $x = 1$. In either event, $G(x)_0 < 0$, so $v_R < 0$ in the vicinity of the conical surface, and v_R may be either positive or negative near the axis. The possibilities are sketched in Fig. 2. Note that the structure of the flow can have one or two cells but no more than two cells is possible.

V. ACCESSIBLE AND NONACCESSIBLE REGIONS OF THE PARAMETER SPACE

In the last section, the structure of the flow was discussed under the assumption that solutions exist. Here we show that in this, as in Ref. 16 there are regions of the parameter space in which solutions fail to exist. Conversely, regions of the parameter space can be exhibited where the existence of solutions is expected.

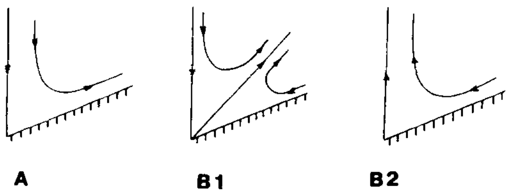

FIG. 2. Streamlines in the meridional plane illustrating the various possibilities for conical vortices.

We have used two equivalent methods to deal with these questions. Garg and Leibovich transformed Eq. (15) to its associated second-order linear equation and used Sturm's comparison theorems. Yih and Wu dealt directly with (15) and we describe their method.

Consider (15), written in the form

$$f' + f^2 = H(x), \tag{32}$$

for two functions $H_1(x)$ and $H_2(x)$, where the corresponding solutions $f_1(x)$ and $f_2(x)$ satisfy the initial condition

$$f_1(x_0) = f_2(x_0) = 0. \tag{33}$$

Then if $H_2(x) \leqslant H_1(x)$, a comparison theorem for equations of the form (32) due to Serrin[16] shows that

$$f_2(x) \leqslant f_1(x). \tag{34}$$

Let us assume that solutions exist, that is, that $f(x)$ is finite in I, and try to determine conditions under which the assumption is tenable or not. Assuming solutions exist, it follows from Sec. IV that $H(x)$ is finite.

A. An upper bound for the solution

Let $H(x)$ be positive in at least a part of the interval I, and suppose $f(x)$ does not approach $-\infty$ in I. Then the integral in (18) exists for all x in I, and $\Omega'(x_0)$ is neither zero nor infinite. That makes $\Omega'(1)$ finite and therefore $H(x)$ finite in I. It then must have a maximum in I. Let it be denoted by $H_{\max}$. Then

$$f < (H_{\max})^{1/2}, \tag{35}$$

and thus f has an upper bound.

For a proof of (35), let f_1 satisfy

$$f_1' + f_1^2 = H_{\max}. \tag{36}$$

The solution of this equation is

$$f_1 = (H_{\max})^{1/2} \tanh(H_{\max})^{1/2} x. \tag{37}$$

Now, since $H(x) \leqslant H_{\max}$, by virtue of the fundamental comparison theorem, $f \leqslant f_1$, and this, taken together with (37), proves (35).

Thus, the nonexistence or existence of the solution of (32) hinges on whether f does or does not become negatively infinite in I.

B. Region of existence of a solution

First, we recall that if $T \geqslant T^*$, then $H(x)$ is nonnegative throughout I. Thus, by virtue of the remarks made in Sec. V A, the existence of fully positive solutions is not contradicted, and we expect to be able to construct solutions for all $T \geqslant T^*$.

For $T < T^*$, f will be negative in the neighborhood of $x = x_0$, and if $|T - T^*|$ is sufficiently large for a given value of Re^2, f may become infinitely negative in I. We shall try to determine a curve in the $\beta - T$ space ($\beta = 0.5\,\pi/\mathrm{Re}$) above which solutions exist.

For this purpose, we consider the lower bounds found in (19) for $G(x)$. This will give us a $G_1(x)$, and hence $H_1(x)$, smaller than their actual values.

From (19), we know that

$$H(x) \geqslant \frac{\mathrm{Re}^2}{(1+x)^2}\left(T + \frac{xI(-x)I(-x_0)}{1-x} - \frac{x_0^2 I(-x_0)}{(1-x_0^2)}\right).$$

The large parentheses have a minimum value at $x = x_0$ when $x_0 < 0$, so

$$H(x) \geqslant \frac{\mathrm{Re}^2}{(1+x)^2}\left(T + \frac{x_0 I(-x_0)}{1-x_0^2}\right). \tag{38}$$

We wish to simplify the calculation by considering a constant lower bound for $H(x)$, and, since we are interested only in those cases where the lower bound is negative, we may weaken (38) by taking

$$H(x) \geqslant H_1 \equiv \frac{\mathrm{Re}^2}{(1+x_0)^2}\left(T + \frac{x_0 I(-x_0)}{1-x_0^2}\right) \tag{39}$$

and assuming that $H_1 < 0$. We now consider

$$f_1' + f_1^2 = H_1, \quad f_1(x_0) = 0, \tag{40}$$

and by the comparison theorem, $f > f_1$. Therefore if a finite solution to (40) exists, a solution to (15) exists. But the solution of (40) for negative H_1 is

$$f_1 = -(-H_1)^{1/2} \tan[(-H_1)^{1/2}(x - x_0)]. \tag{41}$$

This is finite in I if

$$(-H_1)^{1/2} < \pi/2(1 - x_0), \tag{42}$$

or

$$\left(T + \frac{x_0 I(-x_0)}{1-x_0^2}\right)(1+x_0)^{-2} \geqslant -\frac{\beta^2}{(1-x_0)^2}. \tag{43}$$

C. Region of nonexistence of solutions

To show the nonexistence of solutions, we consider upper bounds for $H(x)$ as obtained from (19):

$$H(x) < H_2(x) = \frac{\mathrm{Re}^2}{(1+x)^2}\left(T + \frac{xI(x)}{1-x} - \frac{x_0^2 I(x_0)}{1-x_0^2}\right). \tag{44}$$

Again, we only are concerned with values of $T < T^*$, since otherwise $H(x) > 0$ and existence of solutions is ensured.

Let $f_2(x)$ satisfy

$$f_2' + f_2^2 = H_2(x), \quad f_2(x_0) = 0. \tag{45}$$

We reiterate that solutions to (15) can fail to exist only if $f \to -\infty$ in I. Clearly $H_2(x) \to \infty$ as $x \to 1$, but our strategy is to select a value of $x = x_1 < 1$, and show that there are values of T and Re for which $f_2 \to -\infty$ in the interval $I_1 (x_0 \leqslant x \leqslant x_1)$. By our comparison theorem $f_2 > f$ so $f \to -\infty$ in I as well, and nonexistence of solutions is established. Thus, let x_1 be chosen so that

$$H_2(x_1) = -A^2 < 0. \tag{46}$$

Then

$$f_2 = A \tan A(x - x_0),$$

and $f_2 \to -\infty$ in I, if

$$A(x_1 - x_0) \geqslant \pi/2, \tag{47}$$

or

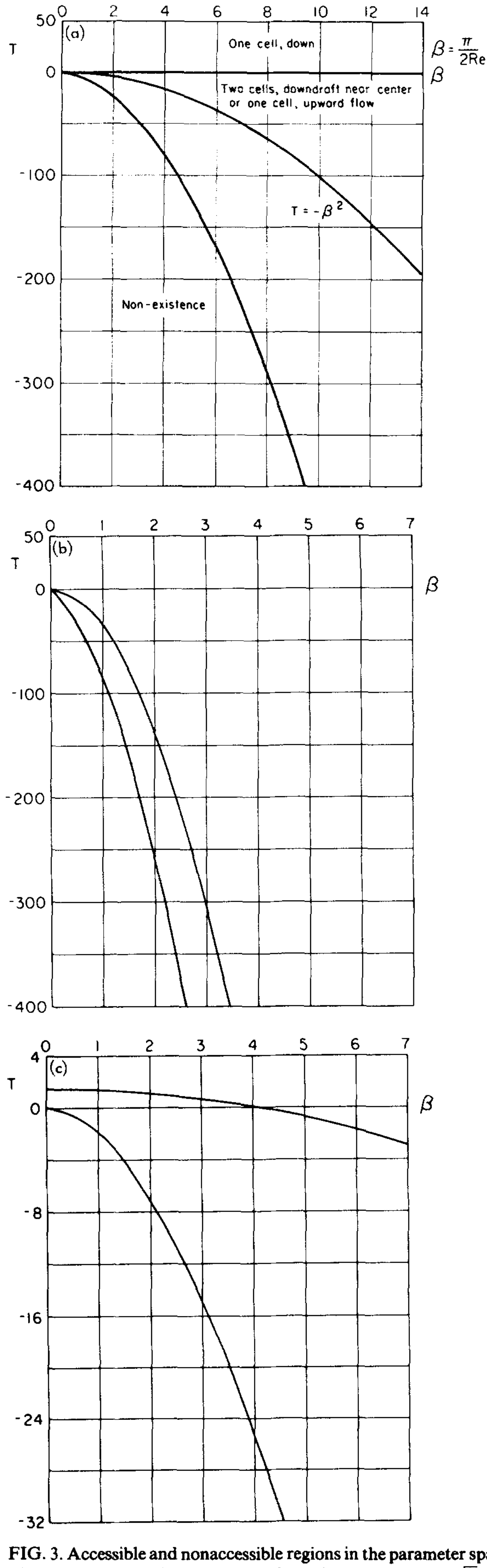

FIG. 3. Accessible and nonaccessible regions in the parameter space (T, Re); (a) when $\phi_0 = \pi/2 (x_0 = 0)$, (b) when $\phi_0 = \pi/4 (x_0 = 1/\sqrt{2})$, (c) when $\phi_0 = 3\pi/4 (x_0 = -1/\sqrt{2})$.

$$-T > \frac{\beta^2(1+x_1)^2}{(x_1-x_0)^2} + \frac{x_1 I(x_1)}{1-x_1} - \frac{x_0^2 I(x_0)}{1-x_0^2}. \qquad (48)$$

The minimum of the right-hand side of (48), taken over x_1 in I, is a function of β and x_0 which we denote by $m(\beta,x_0)$. The equation

$$T = -m(\beta,x_0) \qquad (49)$$

is plotted as the lower curve in each of the Figs. 3(a), 3(b), and 3(c) for $x_0 = 0$, $1/\sqrt{2}$, $-1/\sqrt{2}$, respectively. Below this curve, no solution for f_2 exists, and *a fortiori* no solution for f exists. The upper curves in each of the Figs. 3(a), 3(b), and 3(c) are the loci of points

$$T^* = -\beta^2\frac{(1+x_0)^2}{(1-x_0)^2} - \frac{x_0 I(-x_0)}{1-x_0^2}. \qquad (50)$$

On and above this curve solutions do exist, as seen from the condition (43). In the region between the two curves, our estimates are of no help, and solutions may or may not exist there.

Notice that positive solutions (type A, downward flow) exist for all β (Re). For $\beta \to 0$ (Re $\to \infty$) the region of demonstrated existence for solutions that are negative (type B2, upward flow on axis), or both negative and positive shrinks to zero. The numerical calculations discussed in Sec. VII show that, at least when β is not small, all three types of solution can be found.

VI. NUMERICAL CALCULATIONS

In this section we describe an iterative procedure used to solve numerically the Eqs. (15) and (16) subject to the boundary conditions (17). The method is modeled after a sequence of nested inequalities devised by Ref. 16, who used it both to compute solutions of his problem, and as a tool to prove the existence of solutions to his problem. A similar device was utilized by Weyl[18] to prove the existence of similarity solutions deriving from boundary-layer problems. Serrin's method must, however, be rederived, since the inequalities that he relies upon do not hold directly in the present problem.

Successive approximations were computed by the scheme

$$\Omega_0 \equiv 1,$$

and for $n \geqslant 1$,

$$G_n(x) = 2(1-x)^2\int_{x_0}^{x}\frac{t\Omega_{n-1}^2\,dt}{(1-t^2)^2} + 2x\int_x^1\frac{\Omega_{n-1}^2\,dt}{(1+t)^2} + T(1-x)^2, \qquad (51)$$

$$f_n' + f_n^2 = \frac{Re^2 G_n(x)}{(1-x^2)^2}, \quad f_n(x_0) = 0 \qquad (52)$$

$$\Omega_n'' + 2f_n\Omega_n' = 0, \quad \Omega_n(x_0) = 1, \quad \Omega_n(1) = 0. \qquad (53)$$

If the first two iterates f_1 and f_2 for f were successfully computed, the scheme was found to converge to the solution $(\bar f, \bar\Omega)$. For $x_0 \geqslant 0$, we can prove that it in fact must converge if the solution exists; for $x_0 < 0$, convergence is found numerically in some cases, but our method of proof does not hold.

First we define

$$\bar G(x) = 2(1-x)^2\int_{x_0}^{x}\frac{t\bar\Omega^2\,dt}{(1-t^2)^2} + 2x\int_x^1\frac{\bar\Omega^2\,dt}{(1+t)^2} + T(1-x)^2,$$

and observe that since $\Omega_0 \geqslant \bar\Omega$,

$$G_1 > \bar G,$$

and it follows from our fundamental comparison theorem that $f_1 \geqslant \bar f$.

The next step is to show that $\Omega_1 \leqslant \bar\Omega$. We have the equations

$$\Omega_1'' + 2f_1\Omega_1' = 0,$$

and

$$\bar\Omega'' + 2\bar f\bar\Omega' = 0,$$

with the corresponding boundary conditions,

$$\Omega_1(x_0) = 1, \quad \Omega_1(1) = 0,$$

and

$$\bar\Omega(x_0) = 1, \quad \bar\Omega(1) = 0.$$

Using the fact that both Ω_1' and $\bar\Omega'$ are negative we see that $h = \bar\Omega - \Omega_1$ must satisfy

$$h'' + 2\bar f h' \leqslant 0, \qquad (54)$$

with the boundary conditions $h(x_0) = 0$ and $h(1) = 0$. Equation (54) can be written as

$$\left[h'\exp\left(\int_{x_0}^{x} 2\bar f\,dx\right)\right]' < 0. \qquad (55)$$

Now suppose that $h(x)$ takes on negative values. Then it has a negative minimum at some point $x_m < 1$ where $h'(x_m) = 0$ and $h(x_m) < 0$. Integrating (55) from x_m to $x > x_m$ we obtain $h'(x) \leqslant 0$, which implies that $h(x) < h(x_m)$. This contradicts the boundary condition at $x = 1$ thus proving that $\bar\Omega > \Omega_1$.

Proceeding in the above manner we are led to the nested sequences $\{f_n\}$, $\{\Omega_n\}$ given by

$$f_1 \geqslant f_3 \geqslant \cdots \geqslant \bar f \geqslant \cdots \geqslant f_4 \geqslant f_2,$$

$$\Omega_0 \geqslant \Omega_2 \geqslant \cdots \geqslant \bar\Omega \geqslant \cdots \geqslant \Omega_3 \geqslant \Omega_1.$$

Thus, convergence is assured if a solution corresponding to the chosen values of the parameters Re and T exists and both f_1 and f_2 can be determined.

For some values of the parameters Re and T outside the nonaccessible region discussed in the preceding section, it was found that both f_1 and f_2 could not be computed. It may not, however, be concluded that the failure of the scheme necessarily implies nonexistence of a solution.

Adams predictor–corrector method was used to solve (52) while (53) was integrated by the finite-difference method. Simpson's rule was used for the integrations required to compute $G_n(x)$. Interpolations, wherever necessary, were done by cubic splines. Typically less than 20 iterations were necessary for obtaining the results presented in the next section.

VII. NUMERICAL RESULTS AND DISCUSSION

The method of successive approximations of the previous section was used to generate solutions for three values

TABLE I. The eight examples for which numerical solutions have been obtained.

Case No.	1	2	3	4	5	6	7	8
Re	2	3	100	3	$\sqrt{2}$	3	20	0.5
T	1	1	0	-0.57	-2.2	-0.15	0.1	0.5
x_0	0	0	0	0	0	0	$1/\sqrt{2}$	$-1/\sqrt{2}$

of x_0 corresponding, respectively, to flow over a flat surface, flow within a cone of semi-vertical angle $\pi/4$ and flow over a cone of semi-vertical angle $3\pi/4$. In the case of flow over a flat surface, the values of the parameters Re and T were selected such that all three possible flow patterns (A), (B1) and (B2) (cf. Fig. 2) were obtained.

We are especially interested in cases where $\tilde{\Omega}$ is nearly constant (unity) except in a small region near the axis ($x = 1$) where it rapidly decreases to zero. When this condition exists, $|\tilde{\Omega}'|$ and hence the axial vorticity component, is large near $x = 1$, we say that the flow exhibits boundary layer behavior.

We discuss solutions for the eight cases of Table I. The functions $\tilde{F}$, $\tilde{F}'$, and $\tilde{\Omega}$ are plotted (normalized by taking $\Gamma/2\pi$ equal to unity) in Figs. 4(a), 5(a), ... 11(a), and the corresponding stream surfaces are given in Figs. 4(b), 5(b), ... 11(b).

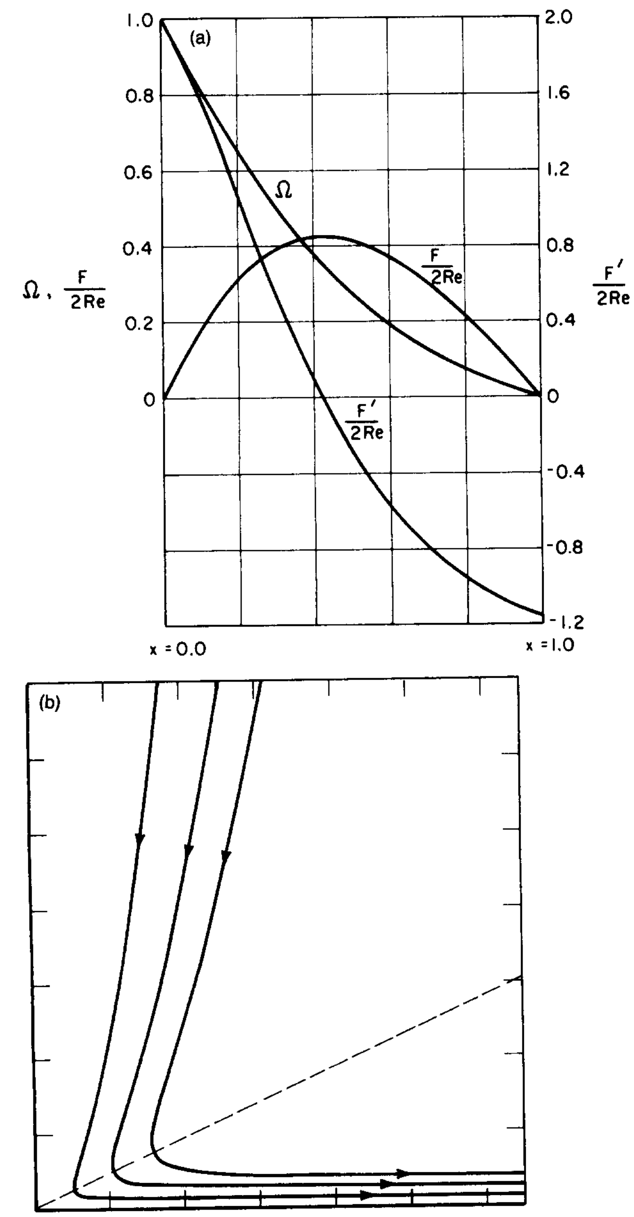

FIG. 4. (a) Numerical solution when Re = 2, $T = 1$, $\phi_0 = \pi/2 (x_0 = 0)$. (b) The resulting flow pattern.

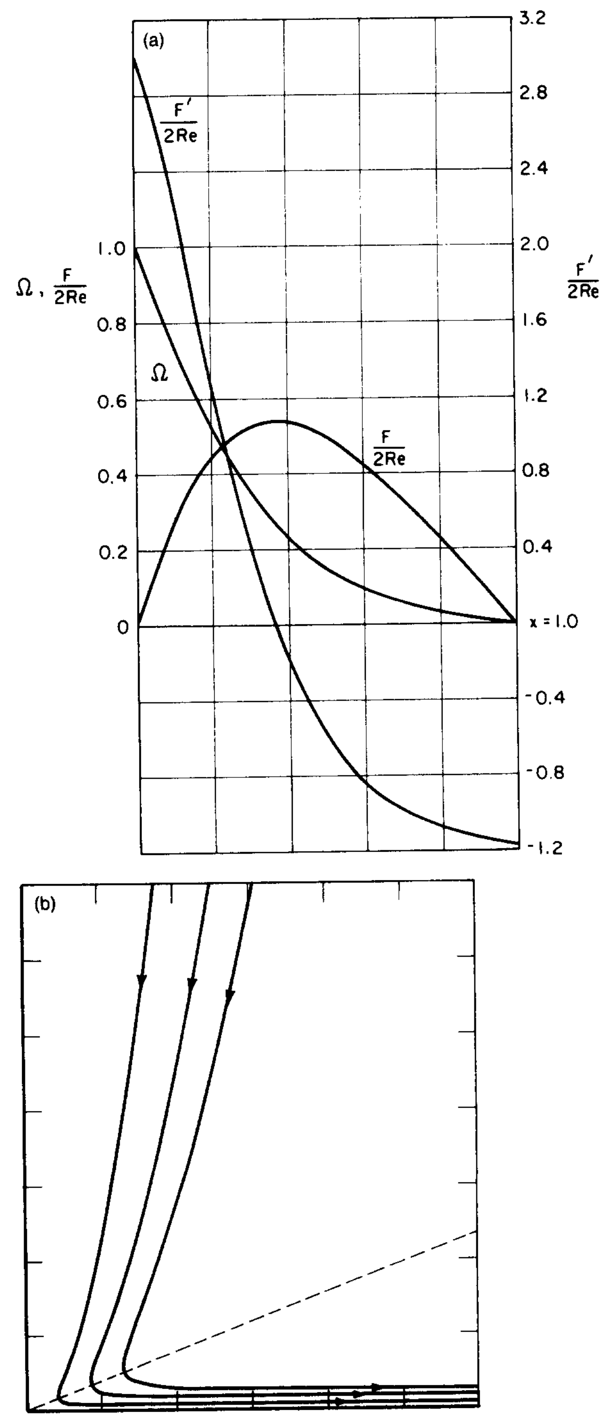

FIG. 5. (a) Numerical solution when Re = 3, $T = 1$, $\phi_0 = \pi/2 (x_0 = 0)$. (b) The resulting flow pattern.

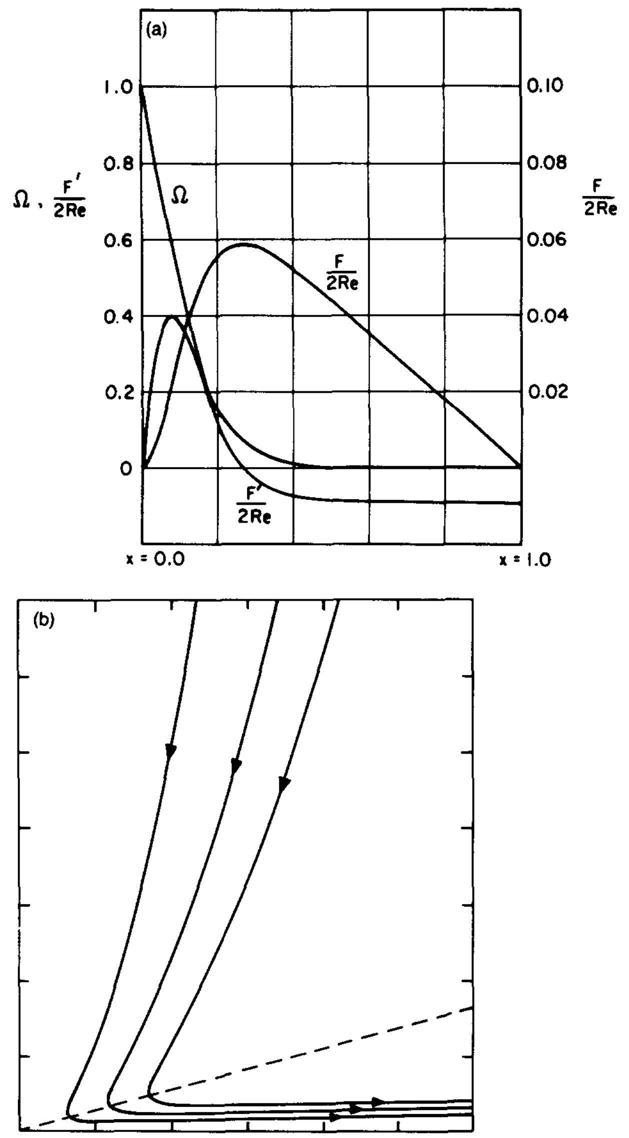

FIG. 6. (a) Numerical solution when $\mathrm{Re} = 100$, $T = 0$, $\phi_0 = \pi/2 (x_0 = 0)$. (b) The resulting flow pattern.

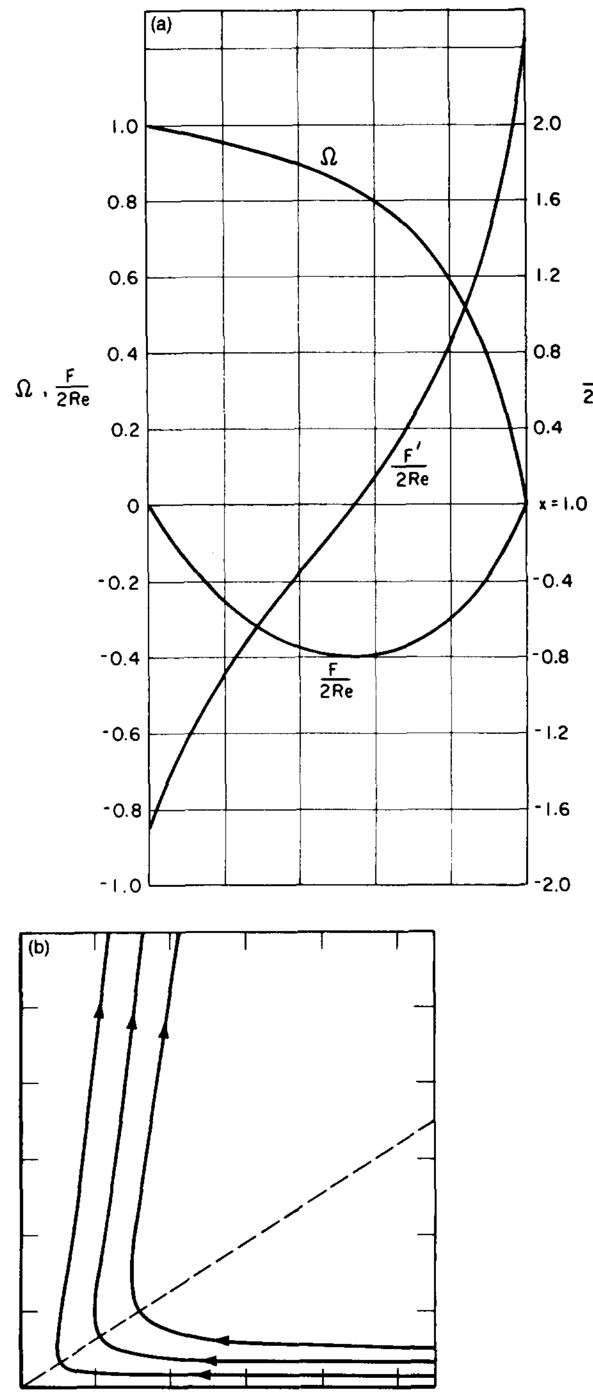

FIG. 7. (a) Numerical solution when $\mathrm{Re} = 3$, $T = -0.57$, $\phi_0 = \pi/2 (x_0 = 0)$. (b) The resulting flow pattern.

The first six cases are for flows above a flat surface ($x_0 = 0$). In cases 1–3, $\widetilde{F} \geqslant 0$ in I. The flow is downward everywhere, with v_ϕ positive. Since $\widetilde{F} \geqslant 0$ and since $\widetilde{\Omega}' < 0$ for all our flows, $\widetilde{\Omega}'' > 0$: thus $\widetilde{\Omega}'$ increases and $|\widetilde{\Omega}'|$ decreases as x increases as is evident in Figs. 4(a), 5(a), and 6(a). Thus no boundary-layer phenomenon for $\widetilde{\Omega}$ can exist near the axis. Notice, however, that strong shear layers form on the boundary $x = x_0 = 0$, and that they are as strong at low Reynolds numbers ($\mathrm{Re} = 3$) as they are at higher ones ($\mathrm{Re} = 100$). There is a correspondingly rapid variation in $\widetilde{\Omega}$ in these cases, and the phenomenon is due to advection of vorticity towards the boundary (since $v_\phi > 0$ throughout the flow).

In cases 4 and 5, $\widetilde{F}$ is entirely negative (except at $x = 0$ and $x = 1$), and so is f, so that $|\widetilde{\Omega}'|$ increases as x increases, as indicated by (18). That is shown in Figs. 7(a) and 8(a). In Fig. 7(a) the increase of $|\widetilde{\Omega}'|$ is fairly gradual, but already indicates the possibility of boundary-layer behavior. In Fig. 8(a), boundary-layer behavior for $\widetilde{\Omega}$ is clearly manifested.

In case 6, $\widetilde{F}$ is first negative then positive, as shown in Fig. 9(a). Since near $x = 1$ it is positive and since the minimum value of $\widetilde{F}$ occurs far from $x = 1$, there is no negative f with large $|f|$. In this case there is therefore no boundary-layer behavior for Ω, as indicated in Fig. 9(a). Figure 9(b) shows the two-cell structure of the flow.

Comparing these results with the numerical results of Long,[14] who assumed boundary-layer behavior to start with, we see that in all his graphs for the vertical velocity w, w is either entirely positive (upward flow) or first negative (downdraft near the center) then positive. This is entirely in agree-

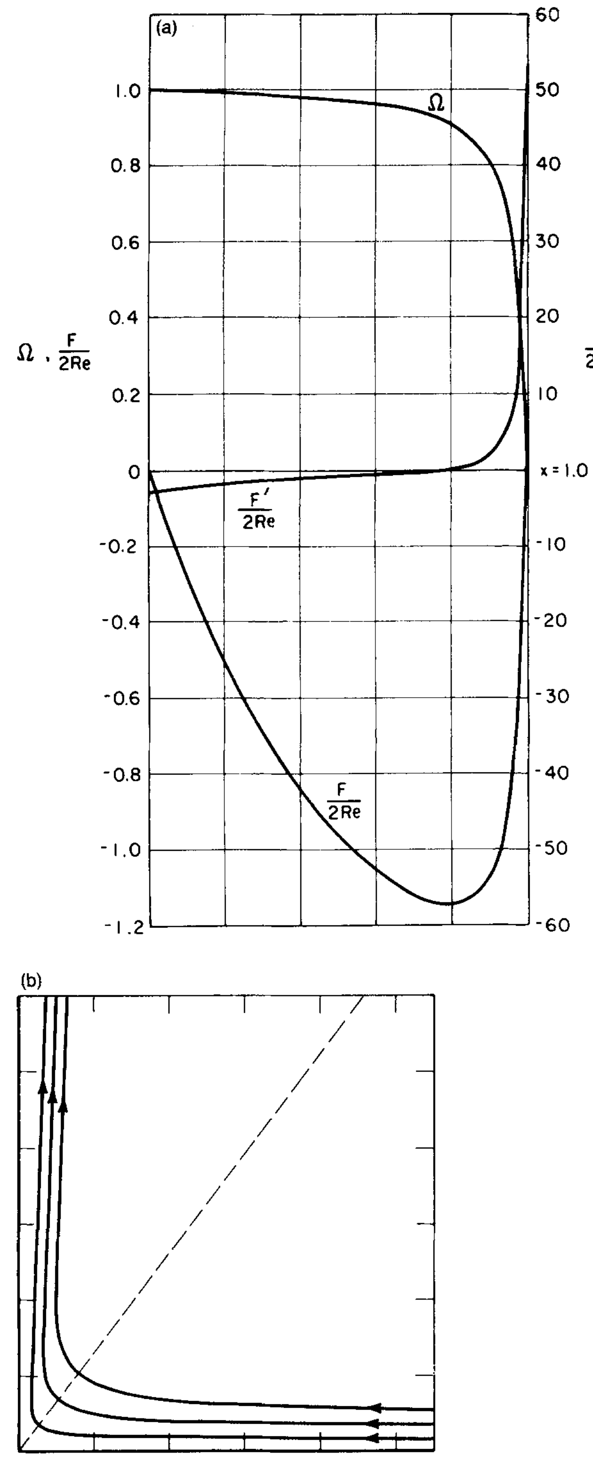

FIG. 8. (a) Numerical solution when $\mathrm{Re} = \sqrt{2}$, $T = -2.2$, $\phi_0 = \pi/2(x_0 = 0)$. (b) The resulting flow pattern.

ment with our deduction that boundary-layer behavior is impossible for positive $\bar{F}(x)$, which corresponds to completely downward flow. Physically, this is due to the fact that vorticity must be advected towards the axis to balance the outward viscous diffusion of vorticity away from the axis that must occur if a concentration of vorticity is to exist near the axis (i.e., if what we have called "boundary-layer behavior" obtains).

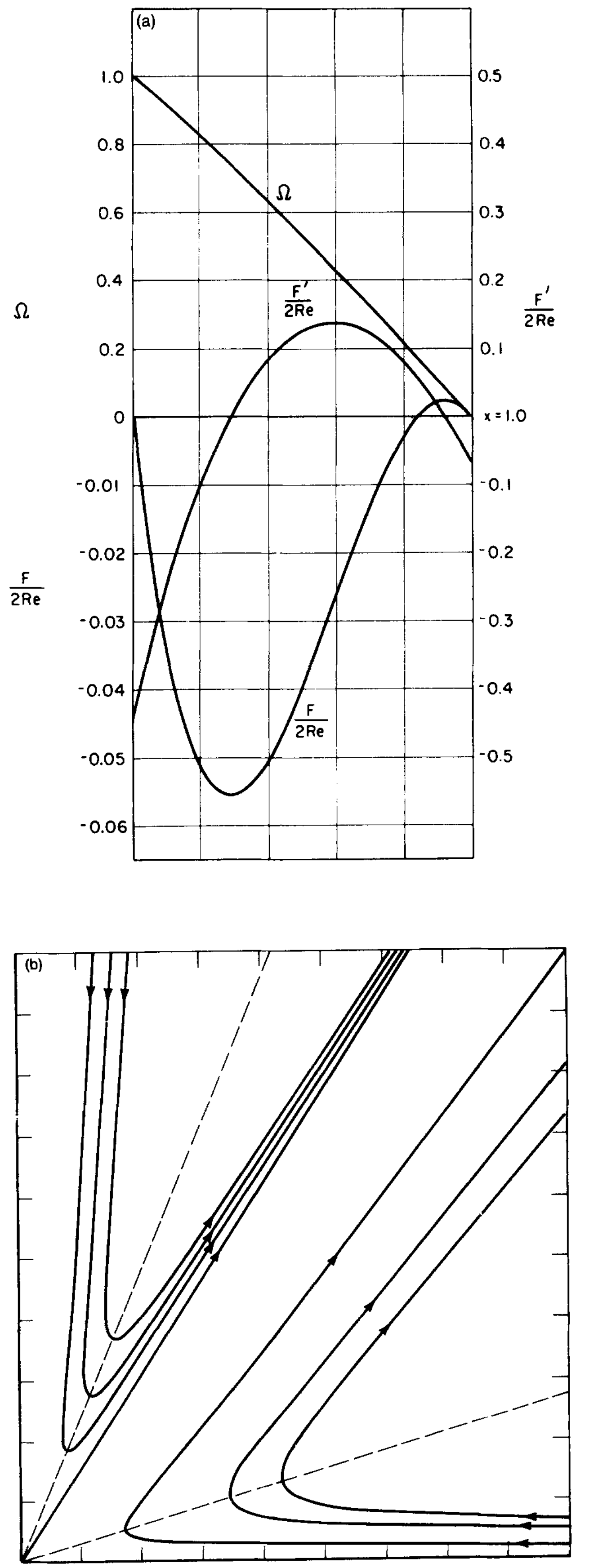

FIG. 9. (a) Numerical solution when $\mathrm{Re} = 3$, $T = -0.15$, $\phi_0 = \pi/2(x_0 = 0)$. (b) The resulting flow pattern.

The results displayed in Fig. 8 are noteworthy: it is remarkable that such a well-developed axial jet and significant concentration of vorticity occur at a low Reynolds number. This behavior has often been observed in experiments at high Reynolds numbers, for instance in the approach flows leading to vortex breakdown. With an increase in the Reynolds number, the axial vorticity should be expected to get further concentrated near the axis. We have been however, unable to find numerical solutions belonging to this class (B2) for values of Re above approximately 4.0. There are two possibilities. It may be that similarity solutions of the assumed form corresponding to the flow pattern B2 do not exist for large Re. It may be, on the other hand, that our numerical scheme, depending, as it does, on the successful computation of the iterates f_1 and f_2 fails to yield these solutions. It is interesting to note that Serrin also was unable to find solutions with upward flow at the axis and radially inward flow on the bounding plane for Re > 2.86.

An example of a flow inside a cone of semi-angle $\pi/4$ ($x_0 = 1/\sqrt{2}$) is shown in Figs. 10 (a) and (b). The flow is of type A, with $\widetilde{F}\geqslant 0$, and is qualitatively similar to the type A

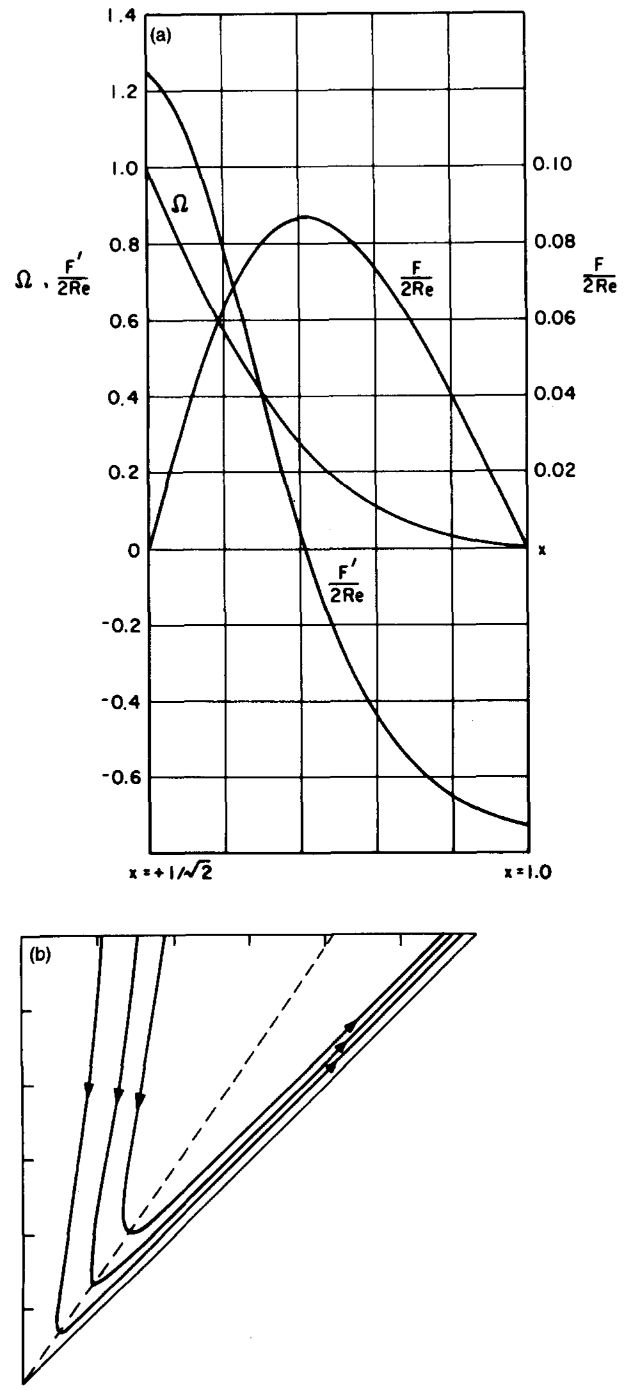

FIG. 10. (a) Numerical solution when Re = 20, $T = 0.1$, $\phi_0 = \pi/4 (x_0 = 1/\sqrt{2})$. (b) The resulting flow pattern.

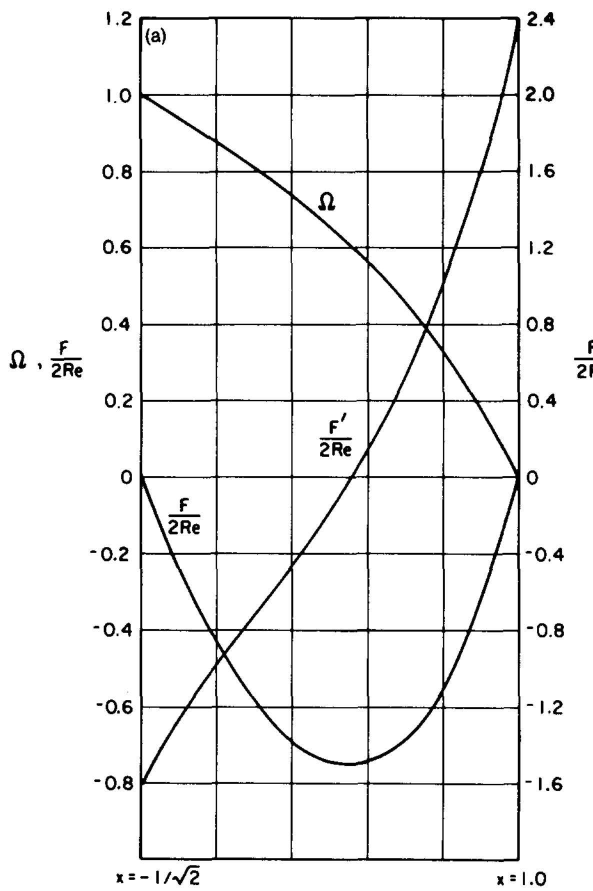

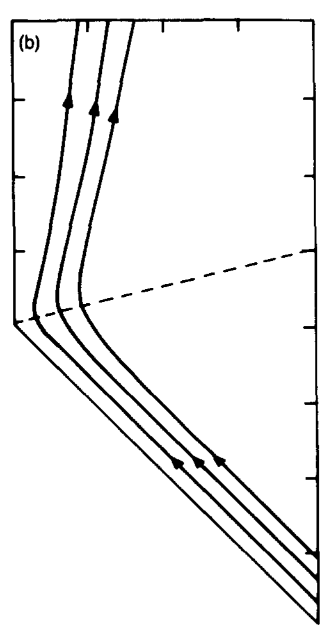

FIG. 11. (a) Numerical solution when Re = 0.5, $T = 0.5$, $\phi = 3\pi/4$ ($x_0 = -1/\sqrt{2}$). (b) The resulting flow pattern.

examples of above a flat surface. Flow *outside* a cone of the same semi-angle (so $\phi_0 = 3\pi/4$ and $x_0 = -1/\sqrt{2}$) is shown in Figs. 11 (a) and (b). The flow is upwards at the axis, or type B2. The Reynolds number is very low (0.5), and the concentration of vorticity near the axis, though in evidence, is weak.

As $x_0 \rightarrow -1$, the cone surface shrinks to a line vortex and the resulting flow may occupy the entire space excluding the negative z axis. In such a situation we have been able to show that $\widetilde{F} \sim (1 + x) \ln(1 + x)$ as $x \rightarrow -1$ and consequently the velocity along the line vortex must be infinite.

We turn next to the violation of the no-slip boundary condition inherent in these solutions. The inability to satisfy all boundary conditions in the presence of realistic (finite) boundaries capable of generating and constraining a viscous fluid motion is a problem that, to our knowledge, is shared by all but *one* known exact solution of the Navier–Stokes equations. (The exception is the trivial one, solid body rotation without relative motion of the fluid and its container: the rest case with zero rotation is a special case.) Exact self-similar solutions may or may not specify bounding surfaces but the region of space occupied by the fluid is always infinite. These solutions are always singular, with unbounded velocities either at a point, a line or at infinity. Each of these solutions represents a flow that can in principle be realized in a finite geometry that excludes the neighborhoods of any singular points provided a special distribution of velocity is arranged at the flow boundaries. Thus, the value of these solutions, so far as applications are concerned, lies in the extent to which portions of the exact solutions resemble flows in finite volumes generated by physically realizable velocity and pressure distributions.

The present solution is a direct generalization of the Squire[10] solution of the round jet. This jet solution improved (or extended) the earlier Landau–Squire[8–9] jet solution which has no boundaries (and, of course no swirl), and placed the flow within conical boundaries. Squire's improved solution, however, failed to satisfy the no-slip condition on the cone, and this condition cannot be remedied according to Squire,[10] Morgan,[21] and Potsch.[22] Schneider[23] has made an attempt to show that this difficulty can be removed within the self-similar framework as $\mathrm{Re} \rightarrow \infty$. It is our view that no-slip probably can be enforced on solutions such as these at high Reynolds numbers, but that this requires at least one of the basic symmetries of the similarity solution to be broken (i.e., it may be *unsteady*, but conical, or steady, but no longer conical). We suspect that higher-order approximations than Schneider's must break the conical similarity. This, however, must be the subject of a later paper.

ACKNOWLEDGMENT

The work of Yih and Wu was supported by the Office of Naval Research, and that of Garg and Leibovich was supported by the National Science Foundation under Grant No. CME 79-191817.

[1]C. duP. Donaldson and R. D. Sullivan, *Proceedings of the 1960 Heat Transfer Fluid Dynamics Institute* (Stanford U.P., Stanford, CA, 1960).

[2]J. M. Burgers, Adv. Appl. Mech. **1**, 197 (1948).

[3]N. Rott, Z. Angew. Math. Phys. **9b**, 543 (1958).

[4]P. G. Bellamy-Knights, J. Fluid Mech. **41**, 673 (1970).

[5]P. G. Bellamy-Knights, J. Fluid Mech. **50**, 1 (1971).

[6]V. Trkal, Cas. Pst. Mat. **48**, 302 (1919).

[7]R. Berker, *Handbuch der Physik*, edited by S. Flügge (Springer-Verlag, Berlin, 1963), Vol. VIII/2.

[8]L. Landau, Dokl. Acad. Sci. U.R.S.S. **43**, 286 (1944).

[9]H. B. Squire, Q. J. Mech. Appl. Math. **4**, 321 (1951).

[10]H. B. Squire, Philos. Mag. **43**, 942 (1952)

[11]H. B. Squire, in *50 Jahre Grenz Schichtforschung*, edited by H. Gortler and W. Tollmien (Braunschweig, 1955).

[12]L. G. Loitsianskii, Prik. Mat. Mekh. **17**, 3 (1953).

[13]R. R. Long, J. Meteor. **15**, 108 (1958).

[14]R. R. Long, J. Fluid Mech. **11**, 611 (1961).

[15]O. R. Burggraf and M. R. Foster, J. Fluid Mech. **80**, 685 (1977).

[16]J. Serrin, Philos. Trans. R. Soc. London Ser. A **271**, 325 (1972).

[17]M. A. Goldstik, Prikl. Mat. Mekh. **24**, 610 (1960).

[18]H. Weyl, Ann. Math. **43**, 381 (1942).

[19]Th. V. Kármán, Z. Angew. Math. Mech. **1**, 233 (1921).

[20]U. T. Bödewadt, Z. Angew. Math. Mech. **20**, 241 (1940).

[21]A. J. A. Morgan, Aeronaut. Q. **7**, 225 (1956).

[22]K. Potsch, Z. Flugwiss. Weltraumforsch. **5**, 44 (1981).

[23]W. Schneider, J. Fluid Mech. **108**, 55 (1981).